Engineered Science

RESEARCH PAPER

View Article Online

Slippery Liquid-infused Porous Surface Fabricated on Aluminum Maintains Stable Corrosion Resistance at Elevated Temperatures

Meng Zhang,[1] Mengyao Dong,[2,3] Shougang Chen*[1] and Zhanhu Guo*[2]

Material corrosion induced by temperature variations is one of the main threats to materials immersed in complex and changeable marine environments. Superhydrophobic surfaces (SHS) are promising for protecting the underlying metal from corrosion. However, temperature variations in underwater environments have hindered the practical application of SHS, thus, their corrosion protection ability is limited. However, slippery liquid infused porous surfaces (SLIPS) can compensate for the aforementioned defects of SHS. In this research, a kind of SLIPS was designed over aluminum for marine corrosion applications using a three-step procedure, consisting of anodization, fluorination and solvent exchange method. The as-prepared SHS and SLIPS were characterized with scanning electron microscopy (SEM), X-ray photoelectron spectroscopy (XPS) and wettability measurement, and their corrosion properties were investigated by electrochemical impedance spectroscopy (EIS). With the perfluorinated lubricant and aluminium oxide coating, the SLIPS presented high corrosion resistance (2.06×10^9 Ω cm^2) in a broad temperature range.

Keywords: Aluminum; EIS; XPS; Slippery liquid infused porous surface; Corrosion protection

Received 30th April 2018, Accepted 26th May 2018

DOI: 10.30919/es8d732

1. Introduction

Aluminum is widely used in shipbuilding and marine pipeline because of its high strength,[1] low density, good corrosion resistance, easy processing molding and many other advantages. Therefore, aluminum has been subjected to achieve more stringent requirements to face the variable and dangerous marine environment. Thus, improved corrosion resistance has been the focus of our research. Previous studies have explored factors that affect corrosion,[2] including acid-base property[3] and air humidity.[4] However, material corrosion induced by temperature variation is seldom studied.

In recently years, superhydrophobic surface (SHS) have been widely used in metal surfaces because of their corrosion resistance.[5] These surfaces mainly consist of rough structure with low surface energy, where the rough surface contains cavities to entrap air to form a stable gas-liquid interface layer to resist entry of corrosive medium.[6] However, the use of SHS for anticorrosion still faces some limitations.[7] For example, when the SHS is immersed into a high-temperature marine environment, the surface tension decreases with increasing temperature of the marine environment. Then the surface hydrophobicity reduces, the air entrapped will slowly be displaced by the external aqueous solution, and corrosion will follow. Thus, a solution is needed to this shortcoming of SHS.

However, slippery liquid infused porous surfaces (SLIPS)[8] can compensate for the aforementioned defects of SHS. Inspired by the Nepenthes pitcher plant, SLIPS[9] had been designed. This surface has recently been considered a promising technology for multifunctional surfaces because it exhibits water-repellency,[10] anti-icing,[11] and antifouling[12] capabilities. In the case of a SLIPS, the fluorocarbon lubricant is infused onto the porous surface of aluminum with a solvent exchange method. Moreover, the injected liquid lubricant can stably be stored in the porous structure with capillary effect[13] and form a continuous, stable, and chemically homogenous liquid interface under the substrate surface even in a high temperature environment. In addition, the liquid lubricant has excellent corrosion resistance. Therefore, SLIPS can be widely applied in anticorrosion applications at various temperatures in marine environments. Thus far, the corrosion inhibition imparted by SHS and SLIPS to metal at different temperatures in marine environments has not been reported.

In this work, we prepared SLIPS-coated Al and investigate this surface corrosion resistance in a simulated marine environment under the temperature range of 293 K to 353 K. For comparison, we also prepared SHS-coated Al. First, a simple anodization method for increasing pore size was developed to construct a rough Al_2O_3 layer on an aluminum surface. SHS-coated Al were designed by fluorination of the rough layer, and a SLIPS-coated Al was fabricated by infusing the lubricant oil into the rough porous structure with solvent exchange method. Their

[1] *College of Materials Science and Engineering, Ocean University of China, Qingdao, 266100, China. E-mail: sgchen@ouc.edu.cn*
[2] *Integrated Composites Laboratory (ICL), Department of Chemical & Biomolecular Engineering, University of Tennessee, Knoxville, TN 37996, USA. E-mail: zguo10@utk.edu*
[3] *School of Materials Science and Engineering, National Engineering Research Center for Advanced Polymer Processing Technology, Zhengzhou University, Zhengzhou, 450002, Henan, China*

surfaces were characterized with scanning electron microscopy (SEM), X-ray photo-electron spectroscopy (XPS), water contact angle (CA) and sliding angle (SA) measurements, and their corrosion properties were investigated by electrochemical impedance spectroscopy (EIS). With the perfluorinated lubricant and aluminium oxide coating, the SLIPS was shown to be able to effectively resist the corrosion caused by the temperature variation. In addition, we explored the effect of temperature on the corrosion behavior of SHS and SLIPS, and observed that the SLIPS presented better relatively stable corrosion resistance than the SHS in different marine environments under the temperature range of 293 K to 353 K.

2. Experimental

2.1. Materials and reagents

Aluminum plates (≥99.99 wt%) are supplied by Beijing Cuibolin Nin-ferrous Technology Developing Co., Ltd, which was cut into 1.0 × 1.0 × 0.2 cm^3. 1*H*,1*H*,2*H*,2*H*-Perfluorodecyltriethoxsilane (PFDS, 97%, Aldrich Inc.), Vertrel XF and Perfluoropolyether (Krytox GPL107. USA) were used as received, other chemical reagents, including phosphoric acid (>85.0%, chemical reagent), acetone (analytical reagent), ethanol (analytical reagent), sodium chloride (analytical reagent) and calcium hydroxide (analytical reagent) were purchased from Sinopharm Chemical Reagent Co., Ltd.

2.2. Fabrication of SHS and SLIPS

2.2.1. Pretreatment. The aluminum foil (1.0 × 1.0 × 0.2 cm^3) was successively washed with acetone, ethanol, and a deionized water solution for 20 min. Then, taken out and dried in nitrogen stream. The cleaned aluminum substrate was anodized in phosphoric acid (5 wt%) to fabricate rough porous microstructure in a two-electrode cell in which the aluminum substrate was employed as a working electrode and a graphite electrode was used as a counter electrode, Additionally, 150 V was used for the anodization voltage, and 1 °C was used for the anodization temperature. After 1 h of anodization, the sample was removed from the cell and thoroughly cleaned with deionized water. During this process, the electrolyte was stirred. To further increase the roughness of the aluminum surface, the anodized aluminum was immersed in a phosphoric acid solution (5 wt%) at 35 °C for 45 min, removed and then dried with nitrogen.

2.2.3. Fabrication of SHS and SLIPS on aluminum plate.

Super hydrophobic surface (SHS):[14] The prepared samples were immersed into 1 vol.% PFDS/ethanol solution for 30 min, then removed and heated in an oven (130 °C, 2 h). Afterwards, the samples were successfully modified with a low-surface-energy material (PFDS), which was confirmed in a later test (XPS, CA, SA).

Slippery liquid infused porous surface (SLIPS):[15] After anodization and modification with PFDS, fluorocarbon lubricant (Krytox GPL107) was infused onto the porous surface of aluminum with a solvent exchange method. The prepared aluminum sheet with porous Al_2O_3 structures was immersed in ethanol, after 10 min, the sample was immediately immersed in Vertrel XF for 10 min, and then the sample was immersed in fluorocarbon lubricant for 20 min. Through the above steps, the solvents were successively replaced until the pores were fully filled with the fluorocarbon lubricant. Eventually, the fluorocarbon lubricant can be storage in the porous structure to resist the entry of corrosive media, what's more, the samples were tilted an angle (~15°) to remove the excess lubricant. The preparation of SHS-coated Al and SLIPS-coated Al is simply shown in Fig. 1.

2.3. Surface characterization

The surface morphology for samples was examined by the scanning electron microscopy (SEM, Hitachi, Japan). The chemical compositions of the films were further investigated by the X-ray photoelectron spectroscopy (XPS: PHI-5702 multifunctional spectrometer using Al Ka radiation). The water contact angles and sliding angles were measured with a contact-angle meter (JC2000D3, Shanghai Zhongchen Digital Technic Apparatus Co., Ltd.) at room temperature. The volume of the water droplet in water contact angle (CA) and sliding angle (SA) measurements was controlled at 5 μL, and most of all, each measurement was the average of around six values made on different areas of surface.

2.4. Electrochemical measurements

The electrochemical tests were performed using Gamry (RFE 2000, USA) in 200 ml 3.5 wt% NaCl aqueous solution. All electrochemical measurements were carried out in a standard three-electrode system: Ag/AgCl electrode was as reference electrode, a platinum mesh was used as counter electrode, and the aluminum sample was as working electrode. The electrochemical impedance spectroscopy (EIS) experiments were conducted in the frequency range from 100 kHz to 0.01 Hz. Before the EIS measurements, it is indispensable to measure the open circuit potential (OCP) of samples in order to allow stabilization of the primarily corrosion potential.[16] Each test was performed more than 3 times under the same experimental conditions to ensure reproducibility of the test results.

3. Results and discussion

3.1. Microstructure

After the bare Al surface was anodized in an aqueous solution of phosphoric acid, it was covered with a dense layer of porous Al_2O_3. According to the previous researches,[17] we can find that the surface becomes more difficult to be wetted by the liquid with larger roughness on the premise that the surface is not wetted. To further increase the roughness of the aluminum surface,[18] the anodized aluminum was immersed in a phosphoric acid solution (5 wt%) at 35 °C for 45 min. Fig. 2 shows the SEM images of the rough Al_2O_3 layer after anodization and increasing pore size, it can be found that the like jungle and tough porous aluminum oxide structure (approximately 80-120 nm) satisfies the first criterion of an SHS and provides space for lubricant infusion and storage.

3.2. XPS and wettability

To obtain a SHS, modification to produce a low surface energy is the second essential condition.[19] The chemical composition and atomic bonding states of the anodic Al_2O_3 layer modified with PFDS was determined via XPS analysis. Signals of Al 2p, C 1s, O 1s, F 1s, Si 2p are observed in Fig. 3. In the Al 2p core-level spectrum shown in Fig. 3b, which exhibits two binding energies of 73.8 eV and 74.7 eV, the peaks are assigned to Al−O−Al and Al-O-Si,[20] respectively, and Al_2O_3 surface was confirmed to be successfully modified by PFDS. The C 1s spectra (Fig. 3c) exhibit six different peaks at the binding

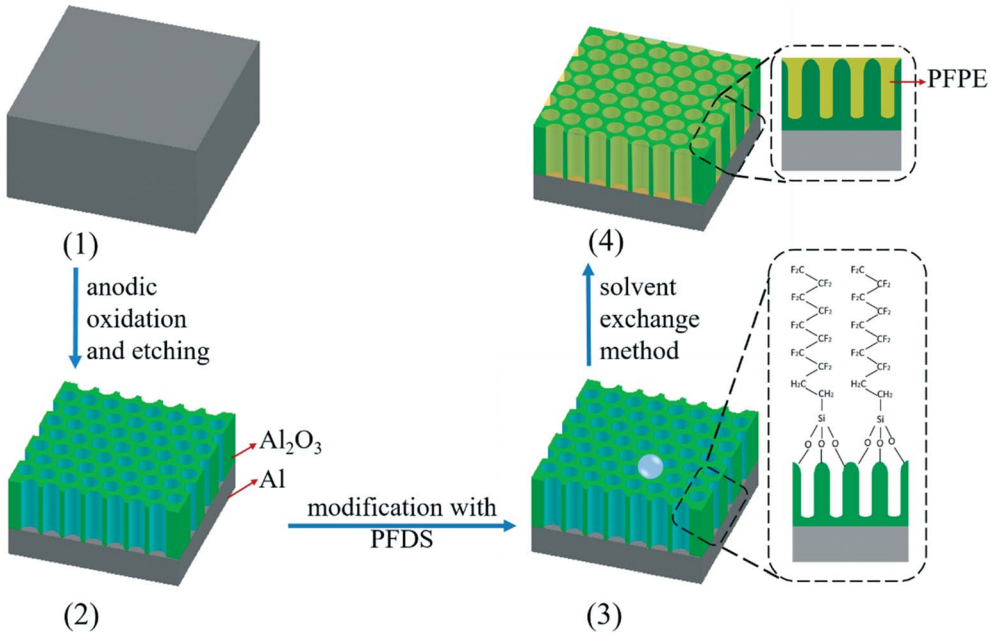

Fig. 1 Schematic illustrations depicting the preparation of SHS-coated Al and SLIPS-coated Al: the pretreated Al substrate[1] was anodized in phosphoric acid (5 wt%) solution at for 1 h at 1 °C and immersed in the same solution at 35 °C for 45 min, after these processes, the aluminum substrate was covered with a dense layer of porous Al_2O_3.[2] Then, the sample was immersed into 1 vol.% PFDS/ethanol solution for 30 min and heated at 130 °C for 2 h, so the SHS-coated Al obtained,[3] in the end, the sample was injected fluorocarbon lubricant by solvent exchange method to fabricate SLIPS-coated Al.[3]

energies of 294.1 ev, 291.6 ev, 289.6 ev, 288.8 ev, 285.5 ev, 283.8 ev, which were respectively assigned to the bonds $-CF_3$, $-CF_2$, $-CH_2-CF_2$,[21] -C-O, -C-C/-C-H, -C-Si,[22–24] the $-CF_3$, $-CF_2$, $-CH_2-CF_2$ came from PFDS. Owing to the low surface energy $-CF_3$ and $-CF_2$ components, the anodic Al_2O_3 layer modified with PFDS is strongly water repellent, as also confirmed in later experiments (CA). The F 1s core-level spectrum was shown in Fig. 3d, and the binding energy of the F 1s peak is 688.7 ev.[25] Fig. 3e shows that the Si 2p spectra exhibit three different peaks at binding energies of 100.8 eV, 102.045 eV, and 103.0 eV, which were assigned to Si–C, Si–O–Al, and Si–O–C bonds, respectively.[24] These results confirm that PFDS was grafted onto the anodic Al_2O_3 surface and are strong evidence of the super hydrophobicity of the aluminum substrate.

The hydrophobic of the films were expressed by the static contact angles of water. Fig. 4 shows the CA of a water droplet on bare Al, SHS. As anticipated, both rough porous structure and modification with PFDS assisted Al_2O_3 layer to show super hydrophobic with a contact angle of 160°. Compared with the bare Al (70°), the SHS exhibited a substantially outstanding surface hydrophobicity, which againconfirms that the low-surface-energy C–F groups were engrafted onto the Al_2O_3 surface.[25] According to Cassie-Baxter model, in case of hydrophobic surface, water droplet contact with not only the solid surface but also the composite interface of solid and gas, the composite plane water contact angle (θ) on the hydrophobic coating can be expressed as follows:[14]

$$\cos\theta = \gamma_f f_{sl} \cos\theta_0 - 1 + f_{sl} \quad (1)$$

where, θ_0 is Young's contact angle on an ideally flat solid surface, γ_f is the roughness of the wetted solid surface, f_{sl} is the fraction of the wetted

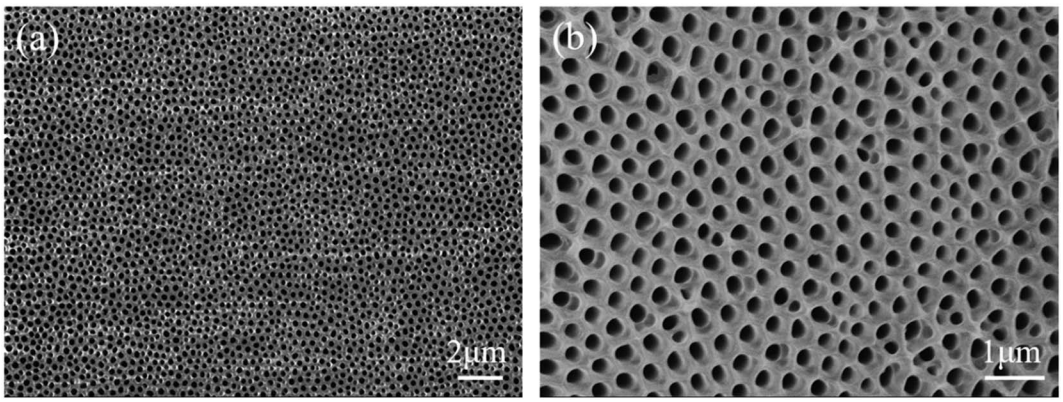

Fig. 2 Surface SEM images with (a) low and (b) high magnification of the aluminum substrate covered with a dense layer of porous Al_2O_3 after anodization and ecthing.

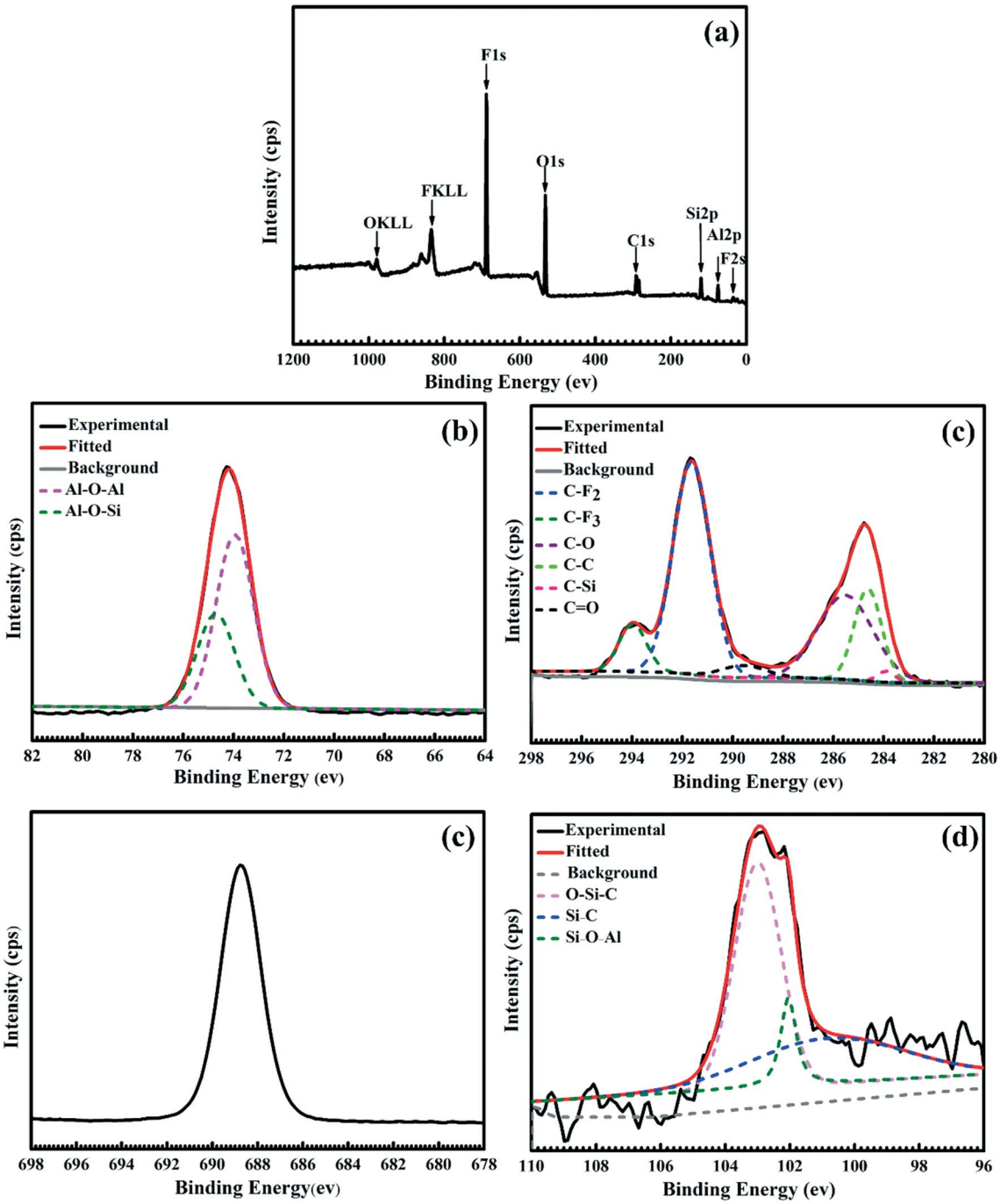

Fig. 3 XPS spectra of the aluminum substrate after anodisation, bearizing and surface modification with PFDS: (a) survey spectrum, (b) Al 2p spectrum, (c) C 1s spectrum, (d) F 1s spectrum, (e) Si 2p spectrum.

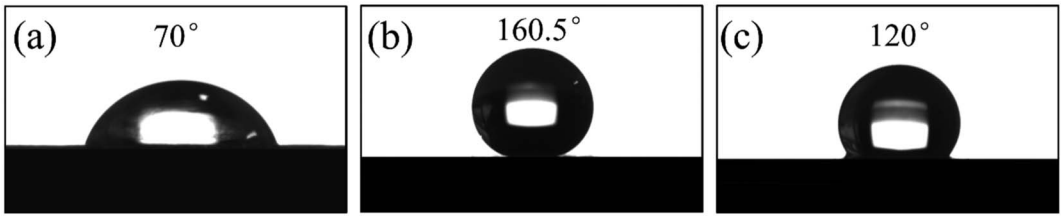

Fig. 4 CA of a water of bare aluminum (a), SHS-coated Al (b) and SLIPS-coated Al (c).

solid surface. From the above Eq. (1), we can find that a low f_{sl} will lead to high water CA on a rough hydrophobic surface. Rough porous structure fabricated on aluminum substrate by anodization and bearizing, after modified with PFDS, the volume of entrapped air reduces the value of f_{sl}, accordingly, the value of θ increases. According to the analysis, it's not difficult to find that the volume of entrapped air improved surface hydrophobicity, thus, the θ increased from 70° to 160°.

When the fluorocarbon lubricant was infused into the rough surface with solvent exchange method, the rough surface of adonic aluminum oxide acted as a reservoir to ensnare the fluorinated lubricant to form a smooth, transparent and static SLIPS on the aluminum substrate.[15] Fig. 4 shows the water CA of a water droplet on SLIPS, owing to the low surface energy of fluorinated lubricant oil, the water CA of the sample increased from 70° to 120°. In summary, the increase of water CA indicated that the lubricant had filled into rough porous structure of the Al_2O_3. In addition, Both SHS and SLIPS exhibited lower sliding angles, As Fig. 5 shows, a water droplet can easily slip down from the SHS and SLIPS with a low titled angle (<10°). In summary, the high water CA and low SA of SHS and SLIPS can explain their high corrosion resistance (shown in the EIS results).

3.3. Study of corrosion protection behavior with electrochemical analysis

3.3.1. EIS results. In order to investigate the corrosion properties of SHS-coated Al and SLIPS-coated Al, EIS was performed in 3.5wt% NaCl aqueous solution. Before EIS, all samples were immersed in a corrosive medium (3.5 wt% NaCl aqueous solution) for more than 5000 s to obtain a relatively steady electrochemical state in the range of ±0.05 V vs.[26] Fig. 6 shows that the Eoc-t curves of bare Al, SHS-coated Al, SLIPS-coated Al in 3.5 wt% NaCl solution at room temperature. It is obvious that the open circuit potentials of three electrodes tend to be stable after immersion for 3000 s. In addition, the more positive potential indicates the decreasing corrosion tendency of the electrode system,[16] the SHS-coated Al and SLIPS-coated Al show the potential trend of corrosion resistance compare to the bare Al, these can be further proved in next EIS results.

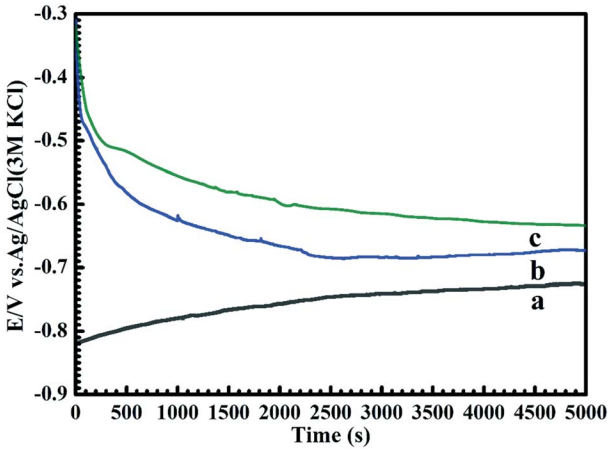

Fig. 6 The >Eoc-t curves of bare Al (a), SHS coated-Al (b), SLIPS-coated Al (c) in 3.5 wt% NaCl solution.

Fig. 7 shows the EIS plots and fitting results of bare Al sample, SHS-coated Al and SLIPS-coated Al in 3.5 wt% NaCl solution at room temperature, in this case, the EIS result for bare Al, SHS coated-Al, SLIPS-coated Al can be respectively analysed with the equivalent circuit (Fig. 7a1, Fig. 7b1, b2), the fitted parameters are summarized in Table 2. As shown in Fig. 7b, the diameter of the capacitive loop in the Nyquist plot of the SHS-coated Al is much larger than that in the Nyquist plot of bare Al (Fig. 7a), in addition, the phase angle of the SHS-coated Al is close to -90° in the low frequency range (Fig. 7b). Furthermore, the impedance at low frequencies is high—on the order of $3.87 \times 10^8\ \Omega\ cm^2$—which is much larger than for the bare Al ($5.3 \times 10^4\ \Omega\ cm^2$). Based on the aforementioned experimental results, the SHS-coated Al can dramatically improve the corrosion resistance of an aluminum sample that is in contact with a NaCl solution at room temperature.

The micro/nano hierarchical structure was fabricated via anodization and increasing pore size. After chemical modification with PFDS, the rough structure acted cavities to entrap air,[27] which can be proved by the CA (Fig. 4), The equivalent circuit used to model the

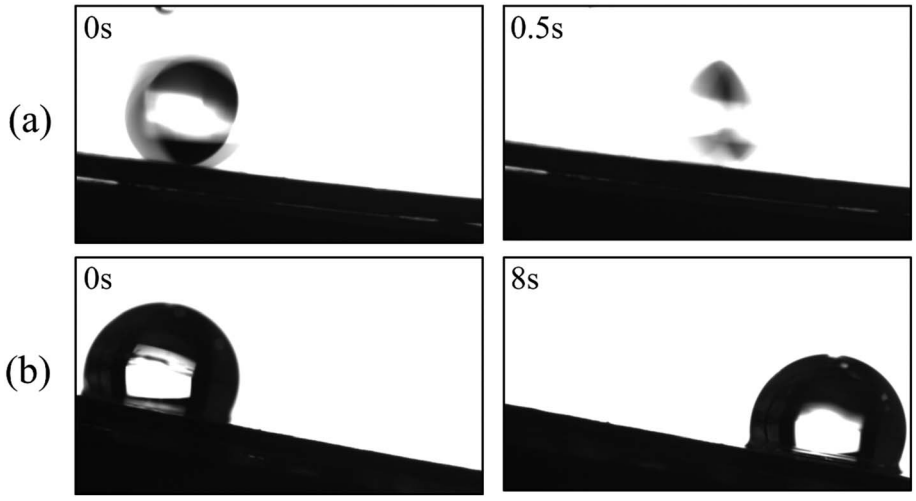

Fig. 5 Dynamic mobility of a water droplet on the SHS-coated Al (a) and SLIPS-coated Al (b) with a low titled angle (<10°).

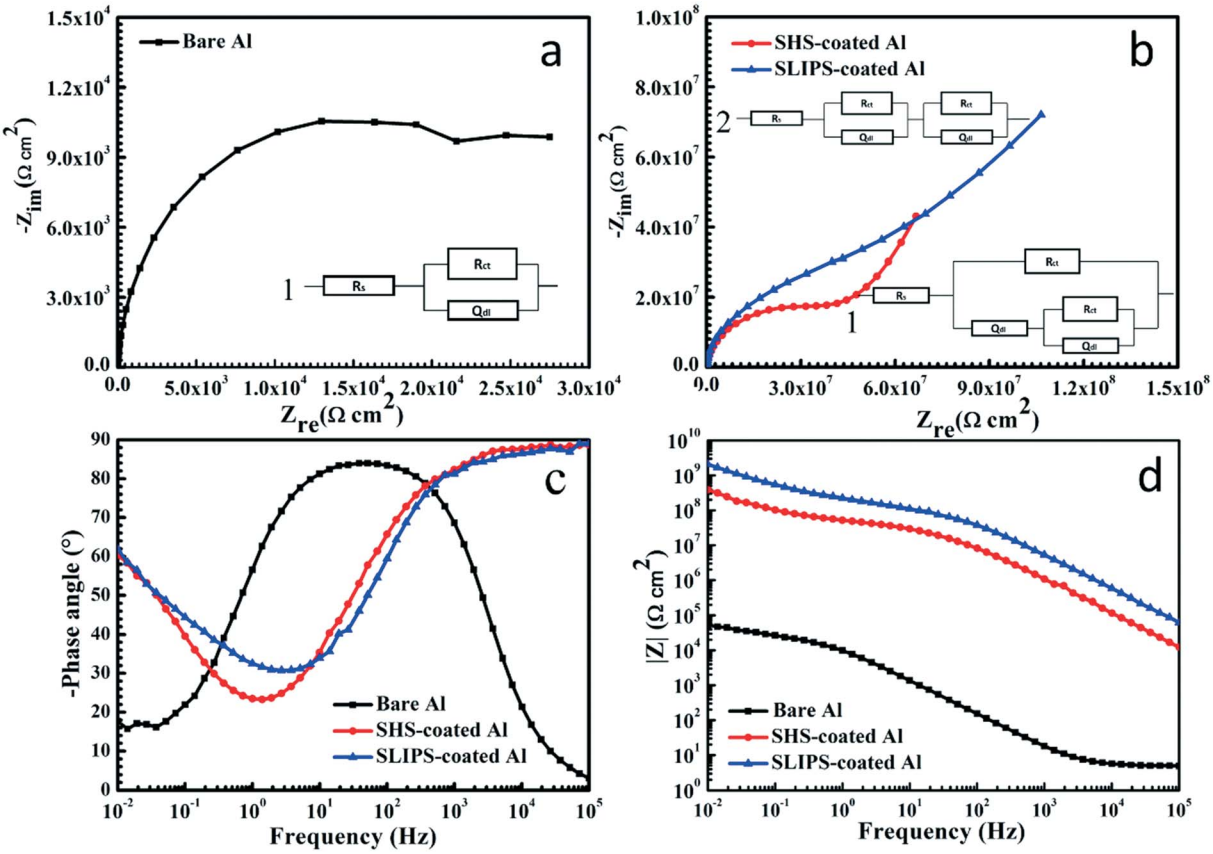

Fig. 7 EIS plots and fitting results of the bare Al sample, the SHS-coated Al and the SLIPS-coated Al in 3.5 wt% NaCl solution at room temperature: (a) (b) Nyquist plots, (c) Bode |Z| versus frequency plots , and (d) Bode-phase angle versus frequency plots. (Equivalent circuits to model the impedance behavior of the bare Al sample (a1), the SHS-coated Al (b1), and the SLIPS-coated Al (b2) in 3.5 wt% NaCl solution).

corresponding impedance spectrum includes two time constants,[5] Thus, the equivalent circuit model for the aluminum surface with super-hydrophobic film was shown in Fig. 7b1 and the fitted parameters are summarized in Table 1. In this equivalent circuit, Rs is the solution resistance, Rc represents the impedance of the super-hydrophobic film, Qc is constant phase element modeling the SHS, Rct describes the impedance of the Al_2O_3 film, Qdl is constant phase element modeling the Al_2O_3 film. As table 1 shows, the high resistance values of both aluminum oxide layer (Rct) and super hydrophobic layer (Rc) indicate that the SHS can protect the underlying aluminum effectively.

3.3.2. EIS evaluation for high-temperature immersion. As previous discussion, temperature is one of the most important factors that affects the corrosion resistance of a metal. We examined the change in corrosion properties for the SHS-coated Al in 3.5 wt% NaCl solution at different temperatures via EIS. Fig. 8 presents (a) Nyquist, (b) Bode |Z| versus frequency plots) and (c) Bode phase angle versus frequency for SHS in 3.5 wt% NaCl at different temperatures (293 K, 313 K, 333 K and 355 K). The equivalent circuit mode is shown in Fig. 7b1 and the fitted parameters are summarized in Table 2. In Fig. 8, the diameter of the capacitive loop and impedance exhibit an obvious steep decrease with an increase in temperature, where a greater diameter of the capacitive loop indicates better corrosion resistance of the material.[28,29] Clearly, the impedance at the lowest temperature is the largest. Moreover, the lower low-frequency impedance modulus |Z| indicates a poorer corrosion protection performance.[30,31] As shown in Fig. 8b, the |Z| value of SHS-coated Al obviously decreases from $3.87 \times 10^8\ \Omega\ cm^2$ to $2.15 \times 10^7\ \Omega\ cm^2$ with an increase of temperature, Thus, the corrosion resistance of SHS-coated Al clearly decreases with increasing temperature, In other words, SHS-coated Al can't maintain a relatively stable corrosion resistance with increasing temperature.

Table 2 shows the electrochemical parameters of SHS coated aluminum in 3.5 wt% NaCl with different temperatures (293 K, 313 K,

Table 1 Electrochemical parameters of the bare Al sample, the SHS-coated Al and the SLIPS-coated Al in 3.5 wt% NaCl solution at room temperature (These parameters are EIS simulation results obtained using the equivalent circuit in Fig. 7. Data are the mean ± standard deviation of at least five replicates.)

Simples	Rct ($\Omega\ cm^2$)	Qdl (F/cm^2)	Rc ($\Omega\ cm^2$)	Qc (F/cm^2)	Rs ($\Omega\ cm^2$)
Bare Al	3.88×10^4	1.71×10^{-5}	----	----	5.4
SHS-coated Al	3.48×10^7	2.69×10^{-10}	1.94×10^8	1.56×10^{-8}	4.3
SlIPS-coated Al	1.90×10^9	2.84×10^{-10}	2.06×10^8	5.87×10^{-11}	4.9

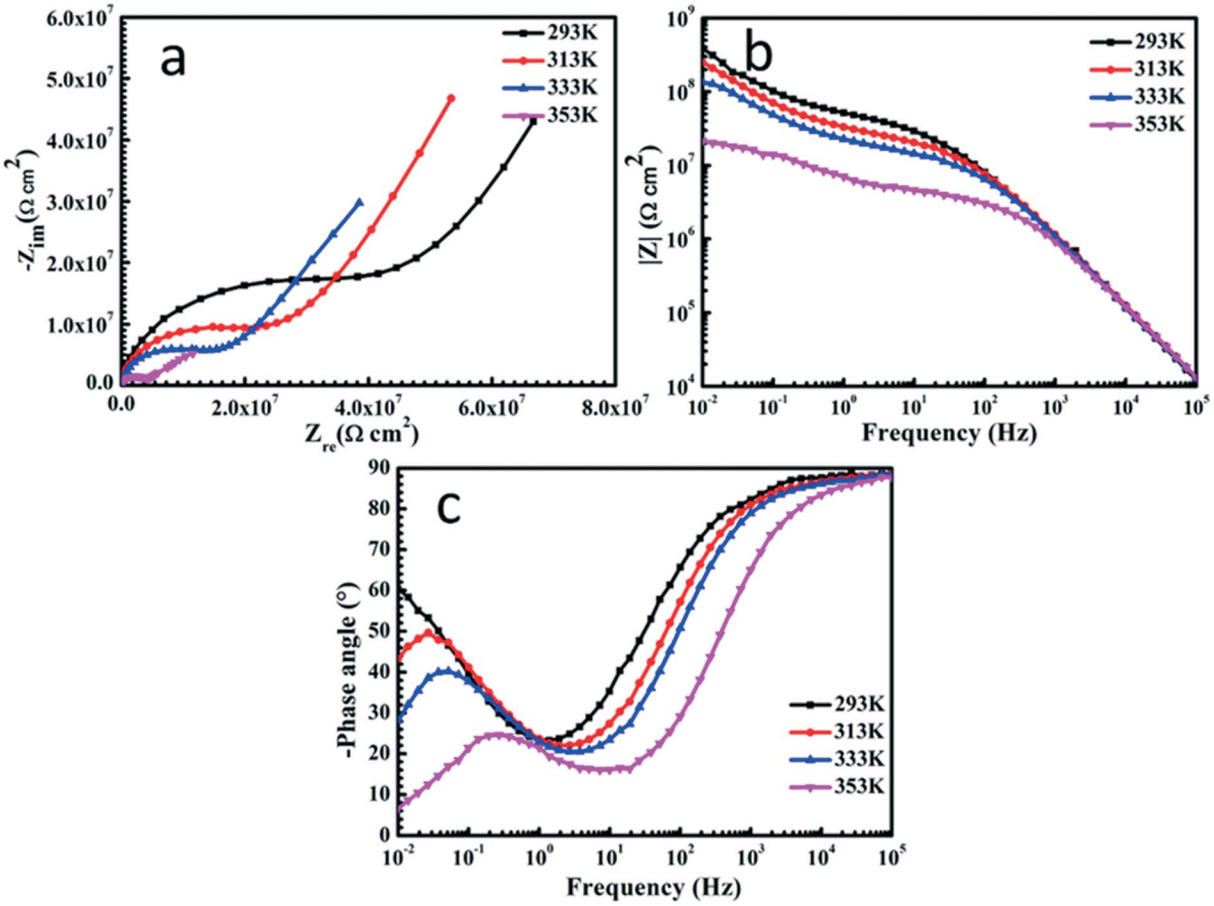

Fig. 8 EIS plots and fitting results of SHS-coated Al in 3.5 wt% NaCl solution at different temperature (293 K, 313 K, 333 K and 353 K): (a) Nyquist plots, (b) Bode |Z| versus frequency plots, and (c) Bode-phase angle versus frequency plots.

333K and 355K). The resistance value of lubricant (Rc) significantly decreases from 1.94×10^8 Ω cm^2 to 1.89×10^7 Ω cm^2 with an increase in temperature. These phenomenon can be attributed to two factors:[1] The relationship between surface tension and water droplet temperature and the relationship between surface tension and contact angle are as follow:[32–34]

$$\gamma = 75.714 - 0.1414t - 0.25399 \times 10^{-3} t^2 \quad (2)$$

$$\cos\theta = (\gamma_{sa} + \gamma_{sl}) / \gamma_{la} \quad (3)$$

Table 2 Electrochemical parameters of SHS-coated Al in 3.5 wt% NaCl solution with different temperature environment (These parameters are EIS simulation results obtained using the equivalent circuit in Fig. 7b. Each data is mean ± standard deviation of at least five replicates.)

Temperature	Rct (Ω cm^2)	Qdl (F/cm^2)	Rc (Ω cm^2)	Qc (F/cm^2)	Rs (Ω cm^2)
293K	3.48×10^7	2.69×10^{-10}	1.94×10^8	1.56×10^{-8}	4.3
313K	1.07×10^7	6.34×10^{-10}	9.97×10^7	4.05×10^{-8}	6.7
333K	8.14×10^6	4.53×10^{-10}	7.62×10^7	6.25×10^{-8}	5.4
353K	6.08×10^6	8.80×10^{-10}	1.89×10^7	3.14×10^{-8}	7.8

where, γ is the surface tension of water at temperature (t), γ_{sa}, γ_{sl}, γ_{la} represent respectively the interfacial surface tensions of solid–air, solid–water and air–water interfacial surface tensions. Considering to the relationship between temperature and surface tension, obviously, the increase of temperature results in the decrease of surface tension of water, on account of Eq. (3), the CA of water will decrease, therefore, the surface wettability of superhydrophobic surfaces is affected by water temperature.[2] When the samples are immersed into a higher temperature environment, the entrapped air will slowly diffuse into the external bulk water,[5] and water enter slowly into the porous structure (as schematic Fig. 10 (a) shows), then give rise to f_{sl} , this will reduce the CA (reference Eq. (1)). Thus, corrosion will follow. The corrosion protection capability of the SHS is limited, in light of the above, these results emphasize the face that the SHS provides high corrosion resistance to corrosive medium, but don't have ability of heat-resistant. To overcome this shortcoming of SHS, in this research, a fluid lubricate was infused onto rough surface of SHS to form SLIPS, we will be discussed the corrosion resistance of SLIPS in different temperature environment.

Noticeably, the injection of fluorocarbon lubricant can effectively enhance the corrosion resistance of the bare Al. As shown in Fig. 7, for the SLIPS-coated Al, the diameter of the capacitive loop in the Nyquist plots represents the impendence of the samples. A larger diameter of the semi-circle for the SLIPS-coated Al demonstrates a higher

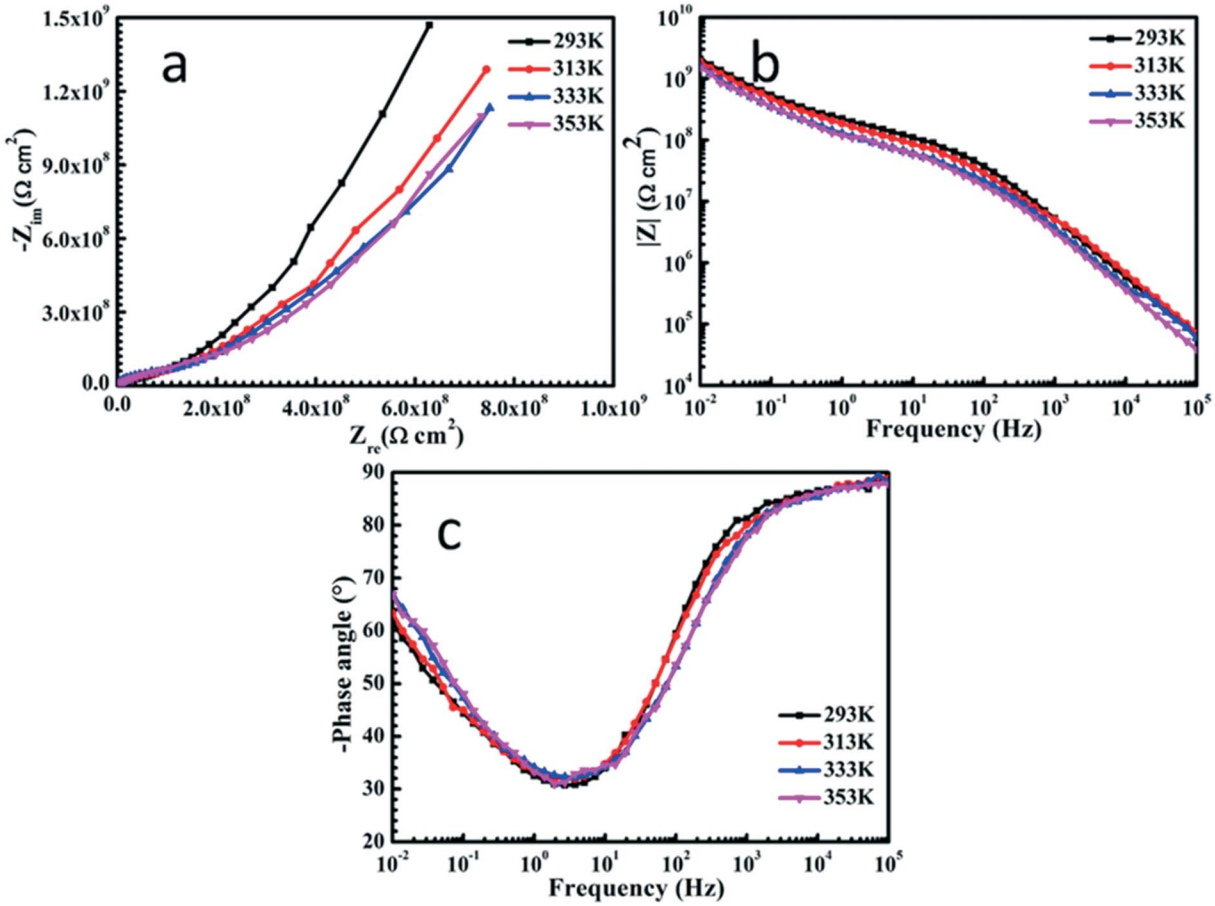

Fig. 9 EIS plots and fitting results of SHS-coated Al in 3.5 wt% NaCl solution at different temperature (293 K, 313 K, 333 K and 353 K): (a) Nyquist plots, (b) Bode-phase angle versus frequency plots, and (c) Bode |Z| versus frequency plots.

impendence compared with that of the SHS-coated Al, indicating that the SLIPS-coated Al films provide greater protection against corrosion. Moreover, the |Z| value of the SLIPS-coated Al is higher than that of the SHS-coated Al, indicating that the presence of SLIPS can further improve the resistance of the substrate to corrosion. These results demonstrate the good barrier properties of the SLIPS-coated Al for inhibiting the penetration of ions (Na^+ and Cl^-) into the aluminum substrate, as shown in the Bode phase plot in Fig. 7b.

To describe the electrochemical behavior of SLIPS-coated Al, we separate it into two oxide phases for purposes of discussion:[35] the barrier layer at the bottom of Al_2O_3 layer and a porous aluminum oxide layer infused with lubricant. The high and medium frequency ranges of EIS results reflect the properties of porous layer infused with lubricant, and the low frequency range corresponds to the barrier layer properties. The properties of each part were characterized by resistances and capacitances in parallel and in series to describe their electronic and dielectric behaviors. Thus, the equivalent circuit model for the SLIPS-coated Al was shown in Fig. 9 and the fitted parameters are summarized in Table 3. In this equivalent circuit model (Fig. 7b2), Rs represents the solution resistance, a parallel branch with resistance Rc and the capacitance Qc characterizes the lubricant infused in the porous Al_2O_3 film, and a parallel branch

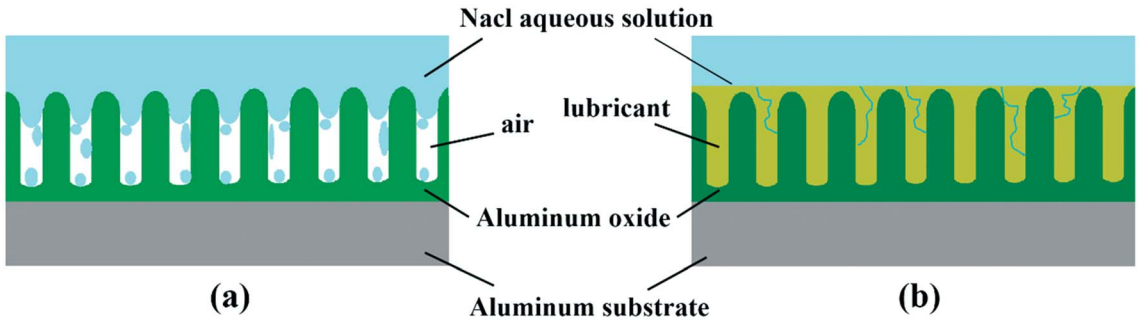

Fig. 10 Schematic of SHS-coated Al and SLIPS-coated Al samples in 3.5 wt% NaCl solution at higher temperature environment.

Table 3 Electrochemical parameters of SHS-coated Al in 3.5 wt% NaCl solution at different temperature environment (These parameters are EIS simulation results with equivalent circuit in Fig. 7c. Each data is mean ± standard deviation of at least five replicates.)

Temperature	Rct (Ω cm^2)	Qdl (F/cm^2)	Rc (Ω cm^2)	Qc (F/cm^2)	Rs (Ω cm^2)
293K	1.90×10^9	2.84×10^{-10}	2.06×10^8	5.87×10^{-11}	4.9
313K	1.53×10^9	1.95×10^{-10}	1.88×10^8	2.79×10^{-11}	6.7
333K	1.29×10^9	1.74×10^{-10}	1.55×10^8	1.42×10^{-11}	7.8
353K	1.02×10^9	1.92×10^{-10}	1.34×10^8	2.44×10^{-11}	5.5

with resistance Rct and the associate capacitance Qct characterizes the barrier layer of Al_2O_3 film.

EIS experiments on SLIPS-coated Al were conducted by immersion in 3.5 wt% aqueous NaCl solution at different temperatures (293 K, 313 K, 333 K and 355 K) (Fig. 9). The equivalent circuits are shown in Fig. 7b2, and the fitted parameters are summarized in Table 3. Similar to the case of SHS-coated Al, the diameter of the capacitive loop and the |Z| value of SLIPS-coated Al showed reduction with the increasing temperature. Unlike the case of SHS-coated Al, the |Z| value of SLIPS-coated Al change little and the Bode phase plot for the SLIPS-coated Al showed low frequency peaks slightly shifted to the right as temperature increased. Table 3 shows the electrochemical parameters of SLIPS-coated Al in 3.5 wt% NaCl for different temperatures. The high resistance values of both barrier layer (Rct) and lubricant (Rc) indicate that the SLIPS-coated Al can effectively protect the underlying Al. When the solution composition is constant, the ion activity on the surface increases with the temperature increases, and the surface corrosion aggravated, so, the resistance value of lubricant (Rc) slightly decreases from 2.06×10^8 Ω cm^2 to 1.34×10^8 Ω cm^2 when the solution temperature was increased from 293 K to 355 K. However, its value at 355 K (2.06×10^9 Ω cm^2) was still substantially higher than the charge transfer resistance of bare Al (3.89×10^4 Ω cm^2) and SHS (3.86×10^8 Ω cm^2), which attributable to the double protection of a dense Al_2O_3 layer and the injection of fluorocarbon lubricant, Thus, the SLIPS exhibits high stability in 3.5 wt% NaCl at the different investigated temperatures. The schematic diagram (Fig. 10b) shows one possible explanation for this phenomenon.[36] SLIPS-coated Al are composed of an Al_2O_3 layer infused with a stable lubricant oil layer, the fluorocarbon lubricant has excellent corrosion resistant property. Thus, the fluorocarbon lubricant with low surface energy can inhibit the penetration of water into the film in the higher environment, and can effectively separate the aluminum substrate and corrosive medium. In addition, the small corrosion followed with the entry of litter water. In general, the injection of a fluorocarbon lubricant will undoubtedly expand the practical application of SHS-coated Al in underwater environment with different temperatures.

4. Conclusions

In summary, SLIPS coating was fabricated on metal aluminum for anticorrosion by two-step procedures. Similarly to SHS-coated Al, the SLIPS-coated Al presented outstanding anticorrosion property at room temperature compared with those of bare Al. In addition, the impedance of the SLIPS-coated Al was higher than that of SHS-coated Al because of the infusion of fluorocarbon lubricants. The fluorocarbon lubricants further resisted the erosion by corrosive medium, functioning as an effective barrier. In contrast to SHS-coated Al, SLIPS-coated Al showed great potential for inhibiting corrosion induced by high temperatures in a 3.5 wt% NaCl aqueous solution. The anticorrosion properties of SHS were substantially diminished with increasing temperature. This phenomenon is explained by the fact that the surface tension decreated and the entrapped air was slowly replaced by the NaCl aqueous solution when the sample was immersed in a high temperature NaCl aqueous solution. Thus, the corrosion would follow. By contrast, the SLIPS-coated Al exhibited stable corrosion resistance in a certain temperature range. The corrosion resistance behavior is attributed to the low surface energy, good thermostability and high corrosion resistance of fluorocarbon lubricants as well as to the porous and compact Al_2O_3 film. The results of this work expand the range of potential applications of SLIPS-covered Al in high-temperature corrosion environments.

Conflicts of interest

There are no conflicts to declare

Acknowledgements

This work was supported by the National Natural Science Foundation (51572249), the Natural Science Foundation for Shandong Province (ZR2014EMM021), the National High Technology Research and Development Programof China (2013A2041106), and the Fundamental Research Funds for the Central Universities (841562011).

References

1 A. Agüero, J. C. D. Hoyo, J. G. D. Blas, M. García, M. Gutiérrez, L. Madueño and S. Ulargui, *Surf. Coat. Tech.*, 2012, **213**, 229–238.
2 J. R. Davis, *Corrosion of Aluminum & Aluminum Alloys*, ASM International, 1999.
3 X. Yang, Z. Sun, D. Wang and W. Forsling, *J. Colloid Interf. Sci.*, 2007, **308**, 395–404.
4 S. E. Stanzl, H. R. Mayer and E. K. Tschegg, *Mat. Sci. Eng. A-Struct.*, 1991, **147**, 45–54.
5 T. He, Y. Wang, Y. Zhang, Q. lv, T. Xu and T. Liu, *Corros. Sci.*, 2009, **51**, 1757–1761.
6 P. Wang, D. Zhang, R. Qiu, J. Wu and Y. Wan, *Corros. Sci.*, 2013, **69**, 23–30.
7 S. Yang, R. Qiu, H. Song, P. Wang, Z. Shi and Y. Wang, *Appl. Surf. Sci.*, 2015, **328**, 491–500.
8 T. V. Charpentier, A. Neville, S. Baudin, M. J. Smith, M. Euvrard, A. Bell, C. Wang and R. Barker, *J. Colloid Interf. Sci.*, 2015, **444**, 81.
9 P. Zhang and F. Y. Lv, *Energy*, 2015, **82**, 1068–1087.
10 X. Liu and J. Liu, *Corros. Sci.*, 2017, **115**, 129–134.
11 P. Kim, T. S. Wong, J. Alvarenga, M. J. Kreder, W. E. Adornomartinez and J. Aizenberg, *Acs Nano*, 2012, **6**, 6569–6577.
12 L. Xiao, J. Li, S. Mieszkin, A. Di Fino, A. S. Clare, M. E. Callow, J. A. Callow, M. Grunze, A. Rosenhahn and P. A. Levkin, *ACS Appl. Mater. Inter.*, 2013, **5**, 10074–10080.
13 P. Wang, D. Zhang and Z. Lu, *Colloid. Surface. B.*, 2015, **136**, 240–247.
14 Z. Lu, P. Wang and D. Zhang, *Corros. Sci.*, 2015, **91**, 287–296.
15 J. Lee, S. Shin, Y. Jiang, C. Jeong, H. A. Stone and C. Choi, *Adv. Funct. Mater.*, 2017, **27**, 1606040.
16 X.-F. Zhang, R.-J. Chen and J.-M. Hu, *Corros. Sci.*, 2016, **104**, 336–343.
17 J. Li, R. Kang, X. Tang, H. She, Y. Yang and F. Zha, *Nanoscale*, 2016, **8**, 7638–7645.
18 L. I. Song-Mei, *Chinese J. Inorg. Chem.*, 2012, **28**, 1755–1762.
19 S. Yuan, Z. Li, L. Song, H. Shi, S. Luan and J. Yin, *ACS Appl. Mater. Inter.*, 2016, **8**, 21214–21220.
20 J. Bing, C. Hu, Y. Nie, M. Yang and J. Qu, *Environ. Sci. Technol.*, 2015, **49**, 1690–1697.

21 W. Peng, H. Li and S. Song, *ACS Appl. Mater. Inter.*, 2017, **9**, 5204–5212.

22 A. Venault, A. J. Jumao-as-Leyba, F.-C. Chou, D. Bouyer, I. J. Lin, T.-C. Wei and Y. Chang, *J. Taiwan Inst. Chem. E.*, 2016, **65**, 459–471.

23 A. Pawbake, V. Waman, R. Waykar, A. Jadhavar, A. Bhorde, R. Kulkarni, A. Funde, J. Parmar, S. Bhattacharyya, A. Date, R. Devan, V. Sharma, G. Lonkar and S. Jadkar, *J. Mater. Sci-Mater. El.*, 2016, **27**, 12340–12350.

24 M. Evaristo, R. Azevedo, C. Palacio and A. Cavaleiro, *Diam. Relat. Mater.*, 2016, **70**, 201–210.

25 S. Tripathi, S. M. Haque, K. D. Rao, R. De, T. Shripathi, U. Deshpande, V. Ganesan and N. K. Sahoo, *Appl. Surf. Sci.*, 2016, **385**, 289–298.

26 D. Zang, R. Zhu, W. Zhang, J. Wu, X. Yu and Y. Zhang, *Corros. Sci.*, 2014, **83**, 86–93.

27 Y. Zhang, S. Tang, J. Hu and T. Lin, *Corros. Sci.*, 2016, **111**, 334–343.

28 H. Zhu, L. Yue, C. Zhuang, Y. Zhang, X. Liu, Y. Yin and S. Chen, *Surf. Coat. Tech.*, 2016, **304**, 76–84.

29 S. Chen, Y. Chen, Y. Lei and Y. Yin, *Electrochem. Commun.*, 2009, **11**, 1675–1679.

30 B. Yin, L. Fang, A. Tang, Q. Huang, J. Hu, J. Mao, G. Bai and H. Bai, *Appl. Surf. Sci.*, 2011, **258**, 580–585.

31 D. Yu, J. Tian, J. Dai and X. Wang, *Electrochim. Acta*, 2013, **97**, 409–419.

32 Q. S. Zheng, Y. Yu and Z. H. Zhao, *Langmuir*, 2005, **21**, 12207–12212.

33 N. J. Shirtcliffe, G. Mchale, M. I. Newton and C. C. Perry, *Langmuir*, 2005, **21**, 937–943.

34 Z. Yu, J. Yang, F. Wan, Q. Ge, L. Yang, Z. Ding, D. Yang, E. Sacher and T. T. Isimjan, *J. Mater. Chem. A*, 2014, **2**, 10639–10646.

35 V. Moutarlier, M. P. Gigandet, B. Normand and J. Pagetti, *Corros. Sci.*, 2005, **47**, 937–951.

36 Y. Wang, H. Zhang, X. Liu and Z. Zhou, *J. Mater Chem. A*, 2016, **4**, 2524–2529.